



Solar cell efficiency tables (Version 63)

Martin A. Green¹  | Ewan D. Dunlop² | Masahiro Yoshita³  |
Nikos Kopidakis⁴ | Karsten Bothe⁵ | Gerald Siefer⁶ | Xiaojing Hao¹

¹Australian Centre for Advanced Photovoltaics, School of Photovoltaic and Renewable Energy Engineering, University of New South Wales, Sydney, 2052, Australia

²European Commission – Joint Research Centre, Ispra, VA, Italy

³Renewable Energy Research Center (RENRC), National Institute of Advanced Industrial Science and Technology (AIST), Central 2, Umezono 1-1-1, Tsukuba, Ibaraki, 305-8568, Japan

⁴National Renewable Energy Laboratory, 15013 Denver West Parkway, Golden, CO, 80401, USA

⁵Calibration and Test Center (CalTeC), Solar Cells Laboratory, Institut für Solarenergieforschung GmbH (ISFH), Emmerthal, Germany

⁶Fraunhofer-Institute for Solar Energy Systems – ISE CalLab, Freiburg, Germany

Correspondence

Martin A. Green, School of Photovoltaic and Renewable Energy Engineering, University of New South Wales, Sydney 2052, Australia.
Email: m.green@unsw.edu.au

Funding information

Australian Renewable Energy Agency, Grant/Award Number: SRI-001; U.S. Department of Energy (Office of Science, Office of Basic Energy Sciences and Energy Efficiency and Renewable Energy, Solar Energy Technology Program), Grant/Award Number: DE-AC36-08-GO28308; Ministry of Economy, Trade and Industry

Abstract

Consolidated tables showing an extensive listing of the highest independently confirmed efficiencies for solar cells and modules are presented. Guidelines for inclusion of results into these tables are outlined and new entries since July 2023 are reviewed.

KEYWORDS

energy conversion efficiency, photovoltaic efficiency, solar cell efficiency

1 | INTRODUCTION

Since January 1993, ‘Progress in Photovoltaics’ has published six monthly listings of the highest confirmed efficiencies for a range of photovoltaic cell and module technologies.^{1–3} By providing guidelines for inclusion of results into these tables, this not only provides an authoritative summary of the current state-of-the-art but also encourages researchers to seek independent confirmation of results and to report results on a standardised basis. In Version 33 of these tables, results were updated to the new internationally accepted reference spectrum (International Electrotechnical Commission IEC 60904–3, Ed. 2, 2008).

The most important criterion for inclusion of results into the tables is that they must have been independently measured by a recognised test centre listed elsewhere.^{1,2} A distinction is made between three different eligible definitions of cell area: total area, aperture area and

designated illumination area, as also defined elsewhere² (note that, if masking is used, masks must have a simple aperture geometry, such as square, rectangular or circular – masks with multiple openings are not eligible). ‘Active area’ efficiencies are not included. There are also certain minimum values of the area sought for the different device types (above 0.05 cm² for a concentrator cell, 1 cm² for a one-sun cell, 200 cm² for a “submodule” and 800 cm² for a module).

In recent years, approaches for contacting large-area solar cells during measurement have become increasingly complex. Since there is no explicit standard for the design of solar cell contacting units, in an earlier issue,³ we describe approaches for temporary electrical contacting of large-area solar cells both with and without busbars. To enable comparability between different contacting approaches and to clarify the corresponding measurement conditions, an unambiguous denotation was introduced and used in subsequent versions of these tables.

This is an open access article under the terms of the [Creative Commons Attribution-NonCommercial-NoDerivs](https://creativecommons.org/licenses/by-nc-nd/4.0/) License, which permits use and distribution in any medium, provided the original work is properly cited, the use is non-commercial and no modifications or adaptations are made.

© 2023 The Authors. Progress in Photovoltaics: Research and Applications published by John Wiley & Sons Ltd.

TABLE 1 Confirmed single-junction terrestrial cell and submodule efficiencies measured under the global AM1.5 spectrum (1000 W/m²) at 25°C (IEC 60904-3: 2008 or ASTM G-173-03 global).

Classification	Efficiency (%)	Area (cm ²)	V _{oc} (V)	J _{sc} (mA/cm ²)	Fill factor (%)	Test centre (date)	Description
<i>Silicon</i>							
Si (crystalline cell)	26.8 ± 0.4 ^a	274.4 (t)	0.7514	41.45 ^b	86.1	ISFH (10/22)	LONGi, n-type HJT ⁴
Si (DS wafer cell)	24.4 ± 0.3 ^a	267.5 (t)	0.7132	41.47 ^c	82.5	ISFH (8/20)	Jinko Solar, n-type
Si (thin transfer submodule)	21.2 ± 0.4	239.7 (ap)	0.687 ^e	38.50 ^{d,e}	80.3	NREL (4/14)	Solexel (35 μm thick) ⁵
Si (thin film minimodule)	10.5 ± 0.3	94.0 (ap)	0.492 ^e	29.7 ^{d,f}	72.1	FhG-ISE (8/07)	CSG Solar (<2 μm on glass) ⁶
<i>III-V cells</i>							
GaAs (thin film cell)	29.1 ± 0.6	0.998 (ap)	1.1272	29.78 ^g	86.7	FhG-ISE (10/18)	Alta Devices ⁷
GaAs (multicrystalline)	18.4 ± 0.5	4.011 (t)	0.994	23.2	79.7	NREL (11/95)	RTI, Ge substrate ⁸
InP (crystalline cell)	24.2 ± 0.5 ^h	1.008 (ap)	0.939	31.15 ⁱ	82.6	NREL (3/13)	NREL ⁹
<i>Thin film chalcogenide</i>							
CIGS (cell) (Cd-free)	23.35 ± 0.5	1.043 (da)	0.734	39.58 ^j	80.4	AIST (11/18)	Solar Frontier ¹⁰
CIGSSe (submodule)	20.3 ± 0.4	526.7 (ap)	0.6834	39.55 ^{d,k}	75.1	NREL (5/23)	Avancis, 100 cells ¹¹
CdTe (cell)	21.0 ± 0.4	1.0623 (ap)	0.8759	30.25 ^e	79.4	Newport (8/14)	First Solar, on glass ¹²
CZTSSe (cell)	12.1 ± 0.3	1.066 (da)	0.5379	35.29 ^k	63.6	NPVM (4/23)	IoP/CAS ¹³
CZTS (cell)	10.0 ± 0.2	1.113 (da)	0.7083	21.77 ⁱ	65.1	NREL (3/17)	UNSW ¹⁴
<i>Amorphous/Microcrystalline</i>							
Si (amorphous cell)	10.2 ± 0.3 ^L _h	1.001 (da)	0.896	16.36 ^e	69.8	AIST (7/14)	AIST ¹⁵
Si (microcrystalline cell)	11.9 ± 0.3 ^h	1.044 (da)	0.550	29.72 ⁱ	75.0	AIST (2/17)	AIST ¹⁶
<i>Perovskite</i>							
Perovskite (cell)	25.2 ± 0.8 ^m	1.0347 (da)	1.162	26.39 ⁿ	82.0	Newport (9/23)	Northwestern ¹⁷
Perovskite (minimodule)	22.4 ± 0.5 ^m	26.02 (da)	1.127 ^d	25.61 ^{d,b}	77.6	NPVM (7/22)	EPFLSion/NCEPU, 8 cells ¹⁸
<i>Dye sensitised</i>							
Dye (cell)	11.9 ± 0.4 ^o	1.005 (da)	0.744	22.47 ^p	71.2	AIST (9/12)	Sharp ^{19,20}
Dye (minimodule)	10.7 ± 0.4 ^o	26.55 (da)	0.754 ^d	20.19 ^{d,q}	69.9	AIST (2/15)	Sharp, 7 serial cells ^{19,20}
Dye (submodule)	8.8 ± 0.3 ^o	398.8 (da)	0.697 ^d	18.42 ^{d,r}	68.7	AIST (9/12)	Sharp, 26 serial cells ^{19,20}
<i>Organic</i>							
Organic (cell)	15.2 ± 0.2 ^{h,s}	1.015 (da)	0.8467	24.24 ^c	74.3	FhG-ISE (10/20)	Fraunhofer ISE ²¹
Organic (minimodule)	15.7 ± 0.3 ^s	19.31 (da)	0.8771 ^d	24.37 ^k	73.4	JET (1/23)	ZhejiangU, 7 cells ²²
Organic (submodule)	11.7 ± 0.2 ^s	203.98 (da)	0.8177 ^d	20.68 ^{d,t}	69.3	FhG-ISE (10/19)	ZAE Bayern, 33 cells ²³

Abbreviations: a-Si, amorphous silicon/hydrogen alloy; AIST, Japanese National Institute of Advanced Industrial Science and Technology; (ap), aperture area; CIGS, CuIn_{1-y}Ga_ySe₂; CZTSSe, Cu₂ZnSnS_{4-y}Se_y; CZTS, Cu₂ZnSnS₄; (da), designated illumination area; DS, directionally solidified (including mono cast and multicrystalline); FhG-ISE, Fraunhofer Institut für Solare Energiesysteme; nc-Si, nanocrystalline or microcrystalline silicon; (t), total area.

^aContacting: Front: 9BB, busbar resistance neglecting; Rear: fully metallised, full-area contact.

^bSpectral response and current–voltage curve reported in Version 61 of these Tables.

^cSpectral response and current–voltage curve reported in Version 57 of these Tables.

^dReported on a ‘per cell’ basis.

^eSpectral responses and current–voltage curve reported in Version 45 of these Tables.

^fRecalibrated from original measurement.

^gSpectral response and current–voltage curve reported in Version 53 of these Tables.

^hNot measured at an external laboratory.

ⁱSpectral response and current–voltage curve reported in Version 50 of these Tables.

^jSpectral response and current–voltage curve reported in Version 54 of these Tables.

^kSpectral response and current–voltage curve reported in Version 62 of these Tables.

^lStabilised by 1000 h exposure to 1 sun light at 50°C.

^mInitial performance. References²⁴ and ²⁵ review the stability of similar devices.

ⁿSpectral response and current–voltage curve reported in the present version of these Tables.

^oInitial efficiency. Reference²⁶ reviews the stability of similar devices.

^pSpectral response and current–voltage curve reported in Version 41 of these Tables.

^aSpectral response and current–voltage curve reported in Version 46 of these Tables.

^rSpectral response and current–voltage curve reported in Version 43 of these Tables.

^sInitial performance. References²⁷ and²⁸ review the stability of similar devices.

^tSpectral response and current–voltage curve reported in Version 55 of these Tables.

TABLE 2 ‘Notable exceptions’ for single-junction cells and submodules: ‘Top dozen’ confirmed results, not class records, measured under the global AM1.5 spectrum (1000 Wm^{−2}) at 25°C (IEC 60904-3: 2008 or ASTM G-173-03 global).

Classification	Efficiency (%)	Area (cm ²)	V _{oc} (V)	J _{sc} (mA/cm ²)	Fill factor (%)	Test Centre (date)	Description
<i>Cells (silicon)</i>							
Si (crystalline)	25.0 ± 0.5	4.00 (da)	0.706	42.7 ^a	82.8	Sandia (3/99)	UNSW, p-type PERC ²⁹
Si (crystalline)	25.8 ± 0.5 ^b	4.008 (da)	0.7241	42.87 ^c	83.1	FhG-ISE (7/17)	FhG-ISE, n-type TOPCon ³⁰
Si (crystalline)	26.0 ± 0.5 ^b	4.015 (da)	0.7323	42.05 ^d	84.3	FhG-ISE (11/19)	FhG-ISE, p-type TOPCon
Si (crystalline)	26.7 ± 0.5	79.0 (da)	0.738	42.65 ^a	84.9	AIST (3/17)	Kaneka, n-type rear IBC ³¹
Si (crystalline)	26.1 ± 0.3 ^b	3.9857 (da)	0.7266	42.62 ^e	84.3	ISFH (2/18)	ISFH, p-type rear IBC ³²
Si (large)	24.0 ± 0.3 ^f	244.59 (t)	0.6940	41.58 ^g	83.3	ISFH (7/19)	LONGi, p-type PERC ³³
Si (large)	25.3 ± 0.4 ^h	268.0 (t)	0.7214	42.07 ⁱ	83.4	ISFH (11/21)	Jinko, n-type TOPCon ³⁴
Si (large)	26.6 ± 0.4 ^j	274.1 (t)	0.7513	41.30 ^s	85.6	ISFH (10/22)	LONGi, p-type HJT ³⁵
Si (large)	26.6 ± 0.5	179.74 (da)	0.7403	42.5 ^k	84.7	FhG-ISE (11/16)	Kaneka, n-type rear IBC ³¹
<i>Cells (III-V)</i>							
GaInP	22.0 ± 0.3 ^b	0.2502 (ap)	1.4695	16.63 ^l	90.2	NREL (1/19)	NREL, rear HJ, strained AlInP ³⁶
<i>Cells (chalcogenide)</i>							
CIGS (thin-film)	23.6 ± 0.4	0.899 (da)	0.7671	38.30 ^m	80.5	FhG-ISE (1/23)	Evolar/UppsalaU ³⁷
CdTe (thin-film)	22.4 ± 0.3	0.4497 (da)	0.8996	31.40ⁿ	79.3	NREL (9/23)	First Solar³⁸
CZTSSe (thin-film)	14.9 ± 0.3	0.2694 (da)	0.5554	36.93 ^m	72.5	NPVM (4/23)	loP/CAS ¹³
CZTS (thin-film)	11.4 ± 0.3	0.2039 (da)	0.7458	21.79 ^m	69.9	NPVM (5/23)	UNSW (Cd-free) ³⁹
<i>Cells (other)</i>							
Perovskite (thin-film)	26.1 ± 0.5^{o,p}	0.05127 (da)	1.201	25.73ⁿ	84.6	NPVM (5/23)	USTC⁴⁰
Perovskite (thin-film)	26.1 ± 0.8^o	0.04929 (da)	1.174	26.13ⁿ	85.2	Newport (7/23)	NorthwesternU/UToronto¹⁷
Organic (thin-film)	19.2 ± 0.3 ^q	0.0326 (da)	0.9135	26.61 ^m	79.0	NREL (3/23)	SJTU ⁴¹
Dye sensitised	13.0 ± 0.4 ^r	0.1155 (da)	1.0396	15.55 ^m	80.4	FhG-ISE (10/20)	EPFL ⁴²

Abbreviations: AIST, Japanese National Institute of Advanced Industrial Science and Technology; (ap), aperture area; CIGS, CuIn_{1−y}Ga_ySe₂; CZTSSe, Cu₂ZnSnS_{4−y}Se_y; CZTS, Cu₂ZnSnS₄; (da), designated illumination area; FhG-ISE, Fraunhofer-Institut für Solare Energiesysteme; ISFH, Institute for Solar Energy Research, Hamelin; NREL, National Renewable Energy Laboratory; (t), total area.

^aSpectral response reported in Version 36 of these Tables.

^bNot measured at an external laboratory.

^cSpectral response and current–voltage curves reported in Version 51 of these Tables.

^dSpectral response and current–voltage curves reported in Version 55 of these Tables.

^eSpectral response and current–voltage curve reported in Version 52 of these Tables.

^fContacting: Front: 12BB, busbar resistance neglected; Rear: fully metallised, full area contacting.

^gSpectral response and current–voltage curves reported in Version 57 of these Tables.

^hContacting: Front: 0BB, grid resistance neglecting; Rear: 9BB, full area contacting, highly reflective chuck.

ⁱSpectral response and current–voltage curves reported in the Version 60 of these Tables.

^jContacting: Front: busbar resistance neglecting contacting; Rear: 9BB, grid resistance neglecting contacting, gold plated chuck.

^kSpectral response and current–voltage curves reported in Version 50 of these Tables.

^lSpectral response and current–voltage curve reported in Version 54 of these Tables.

^mSpectral response and current–voltage curves reported in Version 62 of these Tables.

ⁿSpectral response and current–voltage curves reported in the present version of these Tables.

^oStability not investigated. References²⁴ and²⁵ document stability of similar devices.

^pMeasured using 10-point IV sweep with constant voltage bias until current change rate <0.07%/min.

^qLong-term stability not investigated. References²⁷ and²⁸ document stability of similar devices.

^rLong-term stability not investigated. Reference²⁶ documents stability of similar devices.

TABLE 3 Confirmed multiple-junction terrestrial cell and submodule efficiencies measured under the global AM1.5 spectrum (1000 W/m²) at 25°C (IEC 60904-3: 2008 or ASTM G-173-03 global).

Classification	Efficiency (%)	Area (cm ²)	Voc (V)	Jsc (mA/cm ²)	Fill factor (%)	Test Centre (date)	Description
<i>III-V Multijunctions</i>							
5 junction cell (bonded) (2.17/1.68/1.40/1.06/.73 eV)	38.8 ± 1.2	1.021 (ap)	4.767	9.564	85.2	NREL (7/13)	Spectrolab, 2-terminal
InGaP/GaAs/InGaAs	37.9 ± 1.2	1.047 (ap)	3.065	14.27 ^a	86.7	AIST (2/13)	Sharp, 2 term. ⁴³
GaInP/GaAs (monolithic)	32.8 ± 1.4	1.000 (ap)	2.568	14.56 ^b	87.7	NREL (9/17)	LG Electronics, 2 term.
<i>III-V/Si Multijunctions</i>							
GaInP/GaInAsP//Si (bonded)	36.1 ± 1.3^c	3.987 (ap)	3.309	12.70^d	86.0	FhG-ISE (5/23)	FhG-ISE/AMOLF, 2-term.⁴⁴
GaInP/GaAs/Si (mech. stack)	35.9 ± 0.5 ^c	1.002 (da)	2.52/0.681	13.6/11.0	87.5/78.5	NREL (2/17)	NREL/CSEM/EPFL, 4-term. ⁴⁵
GaInP/GaAs/Si (monolithic)	25.9 ± 0.9 ^c	3.987 (ap)	2.647	12.21 ^e	80.2	FhG-ISE (6/20)	Fraunhofer ISE, 2-term. ⁴⁶
GaAsP/Si (monolithic)	23.4 ± 0.3	1.026 (ap)	1.732	17.34 ^f	77.7	NREL (5/20)	OSU/UNSW/SolAero, 2-term ⁴⁷
GaAs/Si (mech. stack)	32.8 ± 0.5 ^c	1.003 (da)	1.09/0.683	28.9/11.1 ^g	85.0/79.2	NREL (12/16)	NREL/CSEM/EPFL, 4-term. ⁴⁵
GaInP/GaInAs/Ge; Si (spectral split minimodule)	34.5 ± 2.0	27.83 (ap)	2.66/0.65	13.1/9.3	85.6/79.0	NREL (4/16)	UNSW/Azur/Trina, 4-term. ⁴⁸
<i>Perov./Si Multijunctions</i>							
Perovskite/Si	33.9 ± 0.3 ^h	1.0044(da)	1.966	20.76 ⁱ	83.0	NREL (9/23)	LONGi, 2-term. ⁴⁹
Perovskite/Si (large)	28.6 ± 1.4 ^h	258.14(t)	1.909	19.11 ⁱ	78.3	FhG-ISE (5/23)	Oxford PV, 2-term. ⁵⁰
Perov.(minimod.)/Si (cell)	28.4 ± 0.7 ^h	63.98(da)	1.21 ^j /1.648	21.9 ^{ij} /14.3	78.7/81.4	AIST (1/23)	Kaneka, 4-term. ⁵¹
<i>Other Multijunctions</i>							
Perovskite/CIGS	24.2 ± 0.7 ^h	1.045 (da)	1.768	19.24 ^f	72.9	FhG-ISE (1/20)	HZB, 2-terminal ⁵²
Perovskite/perovskite	28.2 ± 0.5 ^h	1.038(da)	2.159	16.59 ⁱ	78.9	JET (12/22)	NanjingU/Renshine, 2-term. ⁵³
Perovskite/perovskite (minimodule)	24.5 ± 0.6 ^h	20.25(da)	2.157	14.86 ^k	77.5	JET (6/22)	NanjingU/Renshine, 2-term. ⁵⁴
a-Si/nc-Si/nc-Si (thin-film)	14.0 ± 0.4 ^{lc}	1.045 (da)	1.922	9.94 ^m	73.4	AIST (5/16)	AIST, 2-term. ⁵⁵
a-Si/nc-Si (thin-film cell)	12.7 ± 0.4 ^{lc}	1.000(da)	1.342	13.45 ⁿ	70.2	AIST (10/14)	AIST, 2-term. ⁵⁶
<i>'Notable Exceptions'</i>							
GaInP/GaAs (mqw)	32.9 ± 0.5 ^c	0.250 (ap)	2.500	15.36 ^o	85.7	NREL (1/20)	NREL/UNSW, multiple QW
GaInP/GaAs/GaInAs	37.8 ± 1.4	0.998 (ap)	3.013	14.60 ^o	85.8	NREL (1/18)	Microlink (ELO) ⁵⁷
GaInP/GaAs (mqw)/GaInAs	39.5 ± 0.5 ^c	0.242 (ap)	2.997	15.44 ^p	85.3	NREL (9/21)	NREL, multiple QW
6 junction (monolithic) (2.19/1.76/1.45/1.19/.97/1.7 eV)	39.2 ± 3.2 ^c	0.247 (ap)	5.549	8.457 ^q	83.5	NREL (11/18)	NREL, inv. metamorphic ⁵⁸
GaInP/AlGaAs/CIGS	28.1 ± 1.2 ^c	0.1386(da)	2.952	11.72 ^r	81.1	AIST (1/21)	AIST/FhG-ISE, 2-term. ⁵⁹
Perovskite/perovskite	29.1 ± 0.5 ^h	0.0489(da)	2.154	16.51 ⁱ	81.7	JET (12/22)	NanjingU/Renshine, 2-term. ⁵³
Perovskite/organic	23.4 ± 0.8 ^h	0.0552(da)	2.136	14.56 ^s	75.6	JET (3/22)	NUS/SERIS, 2-term.

Abbreviations: a-Si, amorphous silicon/hydrogen alloy; AIST, Japanese National Institute of Advanced Industrial Science and Technology; (ap), aperture area; (da), designated illumination area; FhG-ISE, Fraunhofer Institut für Solare Energiesysteme; nc-Si, nanocrystalline or microcrystalline silicon; (t), total area.

^aSpectral response and current-voltage curve reported in Version 42 of these Tables.

^bSpectral response and current-voltage curve reported in the Version 51 of these Tables.

^cNot measured at an external laboratory.

^dSpectral response and current–voltage curves reported in the present version of these Tables.

^eSpectral response and current–voltage curve reported in Version 57 of these Tables.

^fSpectral response and current–voltage curve reported in Version 56 of these Tables.

^gSpectral response and current–voltage curve reported in Version 52 of these Tables.

^hInitial efficiency. References²⁴ and²⁵ review the stability of similar perovskite-based devices.

ⁱSpectral response and current–voltage curves reported in the present version of these Tables.

^jReported on a ‘per cell’ basis.

^kSpectral response and current–voltage curve reported in Version 61 of these Tables.

^lStabilised by 1000 h exposure to 1 sun light at 50°C.

^mSpectral response and current–voltage curve reported in Version 49 of these Tables.

ⁿSpectral responses and current–voltage curve reported in Version 45 of these Tables.

^oSpectral response and current–voltage curve reported in Version 53 of these Tables.

^pSpectral response and current–voltage curves reported in Version 59 of these Tables.

^qSpectral response and current–voltage curve reported in Version 54 of these Tables.

^rSpectral response and current–voltage curve reported in Version 58 of these Tables.

^sSpectral response and current–voltage curve reported in Version 60 of these Tables.

TABLE 4 Confirmed non-concentrating terrestrial module efficiencies measured under the global AM1.5 spectrum (1000 W/m²) at a cell temperature of 25°C (IEC 60904-3: 2008 or ASTM G-173-03 global).

Classification	Effic. (%)	Area (cm ²)	V _{oc} (V)	I _{sc} (A)	FF (%)	Test Centre (date)	Description
Si (crystalline)	24.7 ± 0.3	17,806 (da)	83.04	6.384 ^a	82.9	NREL (4/23)	Maxeon (112 cells)
Si (multicrystalline)	20.4 ± 0.3	14,818 (ap)	39.90	9.833 ^b	77.2	FhG-ISE (10/19)	Hanwha Q Cells (60 cells) ⁶⁰
GaAs (thin-film)	25.1 ± 0.8	866.45 (ap)	11.08	2.303 ^c	85.3	FhG-ISE (11/17)	Alta Devices ⁶¹
CIGS (Cd-free)	19.2 ± 0.5	841 (ap)	48.0	0.456 ^c	73.7	AIST (1/17)	Solar Frontier (70 cells) ⁶²
CdTe (thin-film)	19.5 ± 1.4	23,582 (da)	227.9	2.622 ^d	76.8	NREL (9/21)	First Solar ⁶³
a-Si/nc-Si (tandem)	12.3 ± 0.3 ^e	14,322 (t)	280.1	0.902 ^f	69.9	ESTI (9/14)	TEL Solar, Trubbach Labs ⁶⁴
Perovskite	18.6 ± 0.7 ^g	809.9 (da)	44.7	0.479 ^h	70.3	JET (5/23)	UtmoLight (39 cells) ⁶⁵
Organic	13.1 ± 0.3 ⁱ	1475.0 (da)	48.10	0.6015 ^j	67.0	NREL (5/23)	Waystech/Nanobit ⁶⁶
<i>Multijunction</i>							
InGaP/GaAs/InGaAs	32.65 ± 0.7	965 (da)	24.30	1.520 ^d	85.3	AIST (2/22)	Sharp (40 cells; 8 series) ⁶⁷
<i>‘Notable Exceptions’</i>							
CIGS (large)	18.6 ± 0.6	10,858 (ap)	58.00	4.545 ^b	76.8	FhG-ISE (10/19)	Miasole ⁶⁸
InGaP/GaAs//Si	33.7 ± 0.7	775 (da)	20.3/2.83	1.25/1.93 ^a	86.5/78.0	AIST (2/23)	Sharp/Toyota TI, 4-term. ⁶⁹
InGaP/GaAs//CIGS	31.2 ± 0.7	778 (ap)	20.3/16.9	1.24/.26 ^a	85.7/59.8	AIST (2/23)	Sharp/Idemitsu, 4-term. ⁶⁹

Abbreviations: a-Si, amorphous silicon/hydrogen alloy; a-SiGe, amorphous silicon/germanium/hydrogen alloy; (ap), aperture area; CIGSS, CuInGaSSe; (da), designated illumination area; Effic., efficiency; FF, fill factor; nc-Si, nanocrystalline or microcrystalline silicon; (t), total area.

^aSpectral response and current voltage curve reported Version 62 of these Tables.

^bSpectral response and current–voltage curve reported in Version 55 of these Tables.

^cSpectral response and current–voltage curve reported in Version 50 or 51 of these Tables.

^dSpectral response and current–voltage curve reported in Version 60 of these Tables.

^eStabilised at the manufacturer to the 2% level following IEC procedure of repeated measurements.

^fSpectral response and/or current–voltage curve reported in Version 46 of these tables.

^gInitial performance. References²⁵ and²⁶ review the stability of similar devices.

^hSpectral response and current–voltage curve reported in Version 57 of these Tables.

ⁱInitial performance. References²⁸ and²⁹ review the stability of similar devices.

^jSpectral response and current–voltage curve reported in Version 45 of these Tables.

Tabled results are reported for cells and modules made from different semiconductors and for sub-categories within each semiconductor grouping (e.g., crystalline, polycrystalline or directionally solidified and thin film). From Version 36 onwards, spectral response information is included (when possible) in the form of a plot of the external quantum efficiency (EQE) versus wavelength, either as absolute values or normalised to the peak measured value. Current–

voltage (IV) curves have also been included where possible from Version 38 onwards.

Highest confirmed ‘one sun’ cell and module results are reported in Tables 1–4. Any changes in the tables from those previously published¹ are set in bold type. In most cases, a literature reference is provided that describes either the result reported, or a similar result (readers identifying improved references are welcome to submit to

TABLE 5 Terrestrial concentrator cell and module efficiencies measured under the ASTM G-173-03 direct beam AM1.5 spectrum at a cell temperature of 25°C (except where noted for the hybrid and luminescent modules).

Classification	Effic. (%)	Area (cm ²)	Intensity ^a (suns)	Test Centre (date)	Description
<i>Single cells</i>					
GaAs	30.8 ± 1.9 ^{b,c}	0.0990 (da)	61	NREL (1/22)	NREL, 1 junction (1 J)
Si	27.6 ± 1.2 ^d	1.00 (da)	92	FhG-ISE (11/04)	Amonix back-contact ⁷⁰
CIGS (thin-film)	23.3 ± 1.2 ^{b,e}	0.09902 (ap)	15	NREL (3/14)	NREL ⁷¹
<i>Multijunction cells</i>					
AlGaInP/AlGaAs/GaAs/GaInAs(3) (2.15/1.72/1.41/1.17/0.96/0.70 eV)	47.1 ± 2.6 ^{b,f}	0.099 (da)	143	NREL (3/19)	NREL, 6 J inv. metamorphic ⁵⁸
GaInP/GaInAs; GaInAsP/GaInAs	47.6 ± 2.6 ^{b,g}	0.0452 (da)	665	FhG-ISE (5/22)	FhG-ISE 4 J bonded ⁷²
GaInP/GaAs/GaInAs/GaInAs	45.7 ± 2.3 ^{b,h}	0.09709 (da)	234	NREL (9/14)	NREL, 4 J monolithic ⁷³
InGaP/GaAs/InGaAs	44.4 ± 2.6 ⁱ	0.1652 (da)	302	FhG-ISE (4/13)	Sharp, 3 J inverted metamorphic ⁷⁴
GaInAsP/GaInAs	35.5 ± 1.2 ^{b,j}	0.10031 (da)	38	NREL (10/17)	NREL 2-junction (2 J) ⁷⁵
<i>Minimodule</i>					
GaInP/GaAs; GaInAsP/GaInAs	43.4 ± 2.4 ^{b,k}	18.2 (ap)	340 ^l	FhG-ISE (7/15)	Fraunhofer ISE 4 J (lens/cell) ⁷⁶
<i>Submodule</i>					
GaInP/GaInAs/Ge; Si	40.6 ± 2.0 ^k	287 (ap)	365	NREL (4/16)	UNSW 4 J split spectrum ⁷⁷
<i>Modules</i>					
Si	20.5 ± 0.8 ^b	1875 (ap)	79	Sandia (4/89) ^l	Sandia/UNSW/ENTECH (12 cells) ⁷⁸
Three Junction (3 J)	35.9 ± 1.8 ^m	1,092 (ap)	N/A	NREL (8/13)	Amonix ⁷⁹
Four Junction (4 J)	38.9 ± 2.5 ⁿ	812.3 (ap)	333	FhG-ISE (4/15)	Soitec ⁸⁰
<i>Hybrid module^o</i>					
4-Junction (4 J)/bifacial c-Si	34.2 ± 1.9 ^{b,o}	1,088 (ap)	CPV/PV	FhG-ISE (9/19)	FhG-ISE (48/8 cells; 4 T) ⁸¹
<i>'Notable Exceptions'</i>					
Si (large area)	21.7 ± 0.7	20.0 (da)	11	Sandia (9/90) ^l	UNSW laser grooved ⁸²
Luminescent Minimodule ^o	7.1 ± 0.2	25 (ap)	2.5 ^p	ESTI (9/08)	ECN Petten, GaAs cells ⁸³
4 J Minimodule	41.4 ± 2.6 ^b	121.8 (ap)	230	FhG-ISE (9/18)	FhG-ISE, 10 cells ⁸⁴

Note: Following the normal convention, efficiencies calculated under this direct beam spectrum neglect the diffuse sunlight component that would accompany this direct spectrum. These direct beam efficiencies need to be multiplied by a factor estimated as 0.8746 to convert to thermodynamic efficiencies.⁸⁵

Abbreviations: (ap), aperture area; CIGS, CuInGaSe₂; (da), designated illumination area; Effic., efficiency; FhG-ISE, Fraunhofer-Institut für Solare Energiesysteme; NREL, National Renewable Energy Laboratory.

^aOne sun corresponds to direct irradiance of 1000 Wm⁻².

^bNot measured at an external laboratory.

^cSpectral response and current-voltage curve reported in Version 60 of these Tables.

^dMeasured under a low aerosol optical depth spectrum similar to ASTM G-173-03 direct.⁸⁶

^eSpectral response and current-voltage curve reported in Version 44 of these Tables.

^fSpectral response and current-voltage curve reported in Version 54 of these Tables.

^gSpectral response and current-voltage curve reported in Version 61 of these Tables.

^hSpectral response and current-voltage curve reported in Version 46 of these Tables.

ⁱSpectral response and current-voltage curve reported in Version 42 of these Tables.

^jSpectral response and current-voltage curve reported in Version 51 of these Tables.

^kDetermined at IEC 62670-1 CSTC reference conditions.

^lRecalibrated from original measurement.

^mReferenced to 1000 W/m² direct irradiance and 25°C cell temperature using the prevailing solar spectrum and an in-house procedure for temperature translation.

ⁿMeasured under IEC 62670-1 reference conditions following the current IEC power rating draft 62670-3.

^oThermodynamic efficiency. Hybrid and luminescent modules measured under the ASTM G-173-03 or IEC 60904-3: 2008 global AM1.5 spectrum at a cell temperature of 25°C. 4-terminal module with external dual-axis tracking. Power rating of CPV follows IEC 62670-3 standard, front power rating of flat plate PV based on IEC 60904-3, -5, -7, -10 and 60891 with modified current translation approach; rear power rating of flat plate PV based on IEC TS 60904-1-2 and 60891.

^pGeometric concentration.

the lead author). Table 1 summarises the best-reported measurements for ‘one-sun’ (non-concentrator) single-junction cells and submodules.

Table 2 contains what might be described as ‘notable exceptions’ for ‘one-sun’ single-junction cells and submodules in the above category. While not conforming to the requirements to be recognised as a class record, the devices in Table 2 have notable characteristics that will be of interest to sections of the photovoltaic community, with entries based on their significance and timeliness. To encourage discrimination, the table is limited to nominally 12 entries with the present authors having voted for their preferences for inclusion. Readers who have suggestions of notable exceptions for inclusion into this or subsequent tables are welcome to contact any of the authors with full details. Suggestions conforming to the guidelines will be included on the voting list for a future issue.

Table 3 was first introduced in Version 49 of these tables and summarises the growing number of cell and submodule results involving high efficiency, one-sun multiple-junction devices (previously reported in Table 1). Table 4 shows the best results for one-sun modules, both single- and multiple-junction, while Table 5 shows the best

results for concentrator cells and concentrator modules. A small number of ‘notable exceptions’ are also included in Tables 3 to 5.

2 | NEW RESULTS

Six new results are reported in the present version of these tables. The first is reported in Table 1 (‘one-sun cells and submodules’). An efficiency of 25.2% is reported for a 1-cm² lead halide perovskite cell fabricated by Northwestern University (Illinois, USA)³⁸ as measured by the Newport PV Lab, a major increase over the 24.35% result in the previous version [1]. Also a correction is reported in the footnote of Table 1 reporting measurement details of the record 26.8% efficient, large-area silicon cell fabricated by LONGi Solar in 2022. These were incorrectly reported in both Versions 61 and 62 as ‘Contacting: Front: 9BB, busbar resistance neglecting; Rear: 9BB, full area contacting, highly reflective chuck’. As correctly described in the main text, this cell was a monofacial cell and the correct measurement details are ‘Contacting: Front: 9BB, busbar resistance

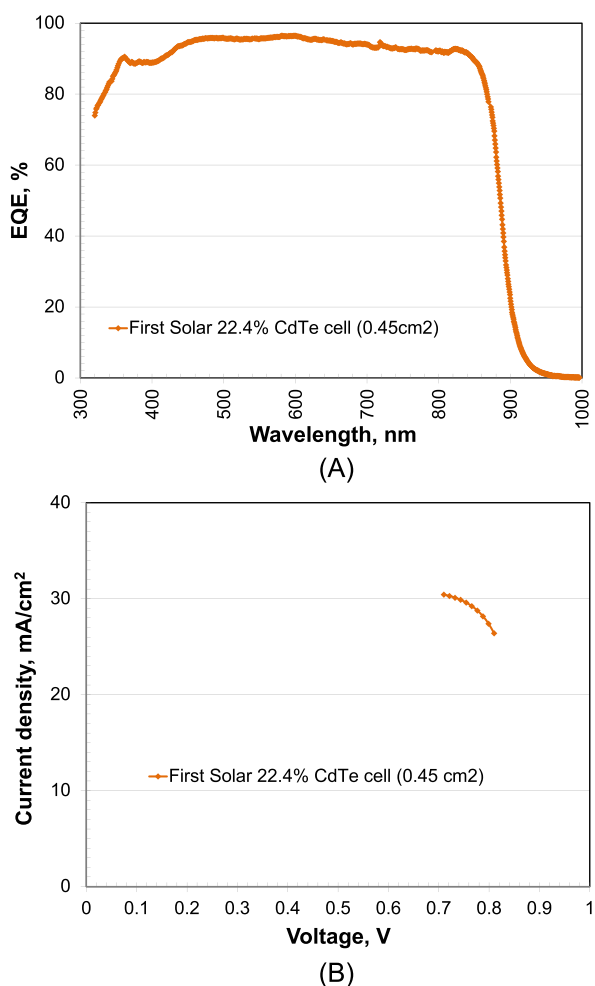


FIGURE 1 (A) External quantum efficiency (EQE) for the new CdTe thin-film cell result reported in this issue. (B) Corresponding current density–voltage (JV) curve.

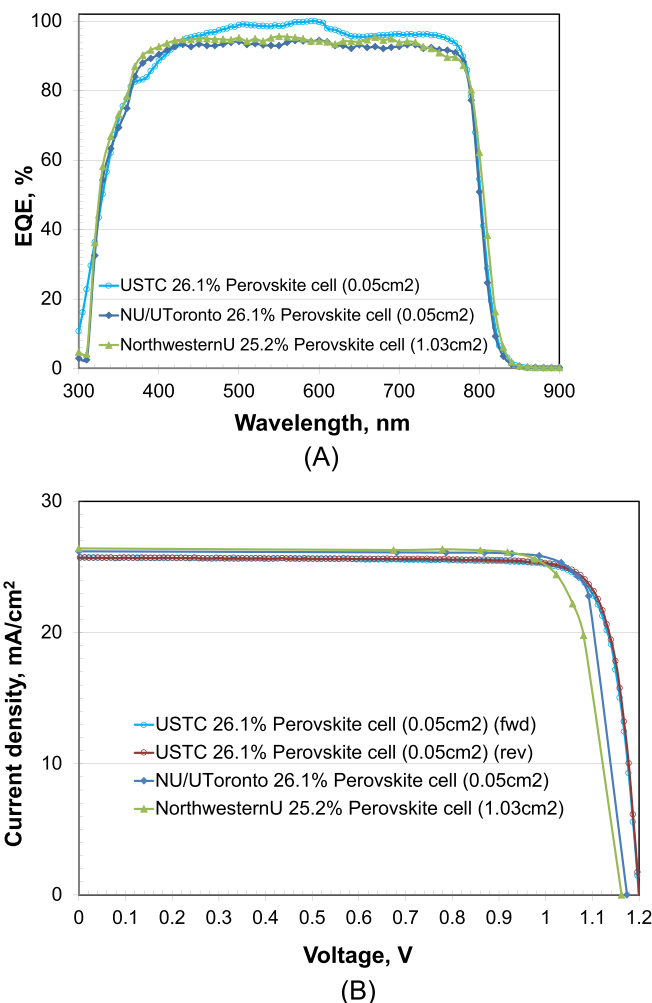


FIGURE 2 (A) External quantum efficiency (EQE) for the new perovskite thin-film cell results reported in this issue (one curve is normalised). (B) Corresponding current density–voltage (JV) curve.

neglecting; Rear: fully metallised, full-area contact'. Please see Version 60 for a full explanation of this terminology.³

Three new results are reported in Table 2 (one-sun 'notable exceptions'), all involving small area, thin-film solar cells. The first is an increase in efficiency to 22.4% for a small area (0.45 cm²) CdTe-based cell fabricated by First Solar³⁸ and measured by the US National Renewable Energy Laboratory (NREL), improving on the 22.3% result reported in the previous version of these tables.¹ The second new result is a similar incremental improvement to 26.1% efficiency for a very small area 0.05 cm² Pb-halide perovskite solar cell fabricated by the University of Science and Technology of China (USTC)⁴⁰ and measured by the Chinese National Photovoltaic Industry Measurement and Testing Center (NPVM).

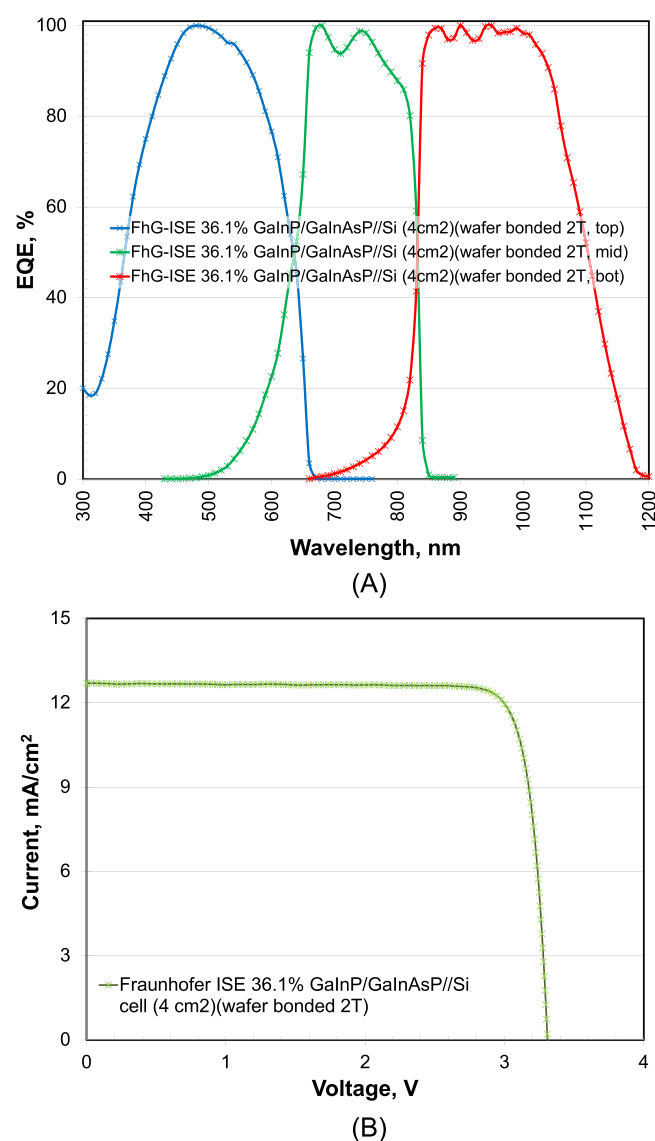


FIGURE 3 (A) External quantum efficiency (EQE) for the new 2-terminal triple-junction GaInP/GaInAsP//Si (wafer bonded) multijunction cell result reported in this issue (results are normalised). (B) Corresponding current density-voltage (JV) curve.

The third new result in Table 2 is the same incremental improvement to 26.1% efficiency again for a very small area 0.05-cm² Pb-halide perovskite solar cell fabricated by Northwestern University in conjunction with the University of Toronto [17] and measured by the Newport PV Lab [1].

For all three results, cell area is too small for classification as an outright record, with solar cell efficiency targets in governmental research programs generally specified in terms of a cell area of 1 cm² or larger.⁸⁷⁻⁸⁹

The fifth new result in this version is reported in Table 3 describing results for one-sun, multijunction devices. An efficiency of 36.1% is reported for a two-terminal, triple-junction GaInP/GaInAsP//Si (wafer bonded) cell fabricated by the Fraunhofer Institute for Solar Energy Systems (FhG-ISE) and AMOLF (Amsterdam)⁴⁴ and measured

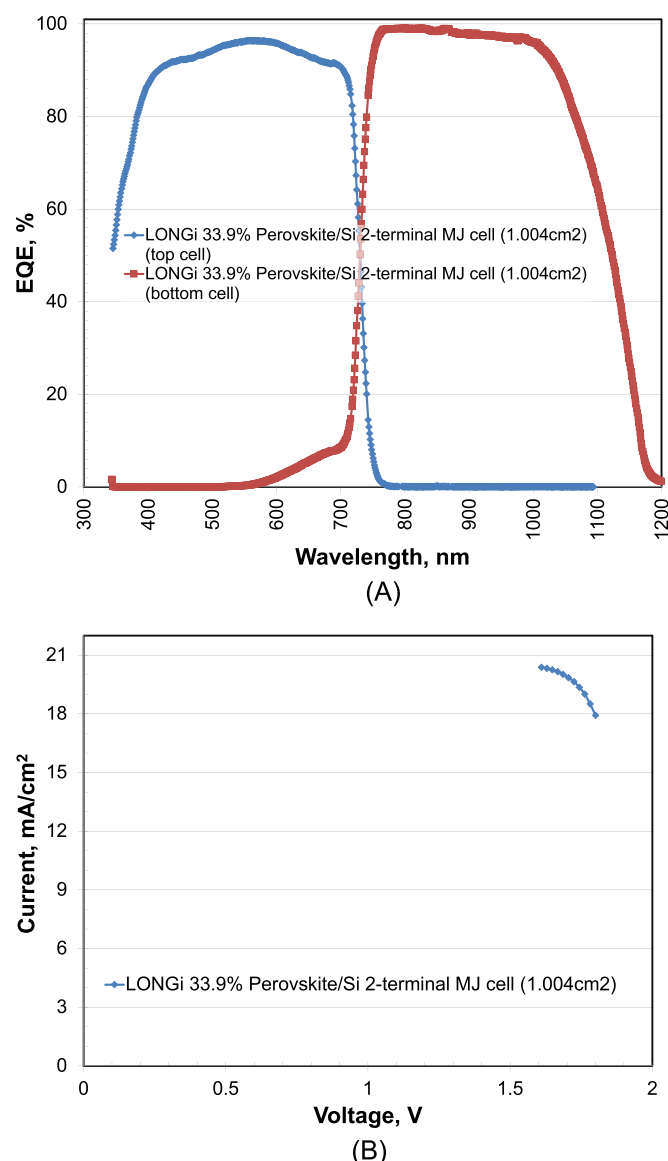


FIGURE 4 (A) External quantum efficiency (EQE) for the new 2-terminal double-junction Perovskite/Si multijunction cell result reported in this issue (results are normalised). (B) Corresponding current density-voltage (JV) curve.

by FhG-ISE. This has been reported as the highest one-sun efficiency ever reached for a solar cell based on silicon. The final new result is 33.9% efficiency for a 1-cm², 2-terminal, double-junction perovskite/Si cell fabricated by LONGi⁴⁹ and measured by NREL.

There are two corrections in Table 4 (one-sun modules) involving two results reported as 'notable exceptions' in the previous version of these tables.¹ The two high efficiency four-terminal modules reported as fabricated by Sharp and measured by AIST should have been reported as being fabricated by Sharp/Toyota-TI and Sharp/Ide-mitsu, respectively.

The EQE spectra for the new CdTe thin-film cell reported in the present issue of these tables are shown in Figure 1(A), with Figure 1(B) showing the current density–voltage (JV) curves for the same device. Figure 2(A) and (B) shows the corresponding EQE and JV curves for the new perovskite thin-film cell results. Figure 3(A) and (B) shows these for the new triple-junction GaInP/GaInAsP//Si (wafer-bonded) multijunction cell result while Figure 4(A) and (B) shows these for the new perovskite/Si 2-terminal, double junction device.

3 | DISCLAIMER

While the information provided in the tables is provided in good faith, the authors, editors and publishers cannot accept direct responsibility for any errors or omissions.

ACKNOWLEDGEMENTS

The Australian Centre for Advanced Photovoltaics commenced operation in February 2013 with support from the Australian Government through the Australian Renewable Energy Agency (ARENA). The Australian Government does not accept responsibility for the views, information or advice expressed herein. The work at NREL was supported by the U.S. Department of Energy under Contract No. DE-AC36-08-GO28308 with the National Renewable Energy Laboratory. The work at AIST was supported in part by the Japanese New Energy and Industrial Technology Development Organisation (NEDO) under the Ministry of Economy, Trade and Industry (METI). Open access publishing facilitated by University of New South Wales, as part of the Wiley - University of New South Wales agreement via the Council of Australian University Librarians.

DATA AVAILABILITY STATEMENT

The data that support the findings of this study are available from the corresponding author upon reasonable request.

ORCID

Martin A. Green  <https://orcid.org/0000-0002-8860-396X>

Masahiro Yoshita  <https://orcid.org/0000-0003-1924-1288>

REFERENCES

- Green MA, Dunlop ED, Yoshita M, Kopidakis N, Siefer G, Hao XJ. Solar cell efficiency tables (version 62). *Prog Photovolt: Res Appl*. 2022; 31(7):651–663. doi:10.1002/pp.3726
- Green MA, Dunlop ED, Siefer G, Yoshita M, Kopidakis N, Hao XJ. Solar cell efficiency tables (version 61). *Prog Photovolt: Res Appl*. 2022; 31(1):3–16. doi:10.1002/pp.3646
- Green MA, Dunlop ED, Hohl-Ebinger J, et al. Solar cell efficiency tables (version 60). *Prog Photovolt: Res Appl*. 2022;30(7):687–701. doi: 10.1002/pp.3595
- Yang M, Ru X, Yin S, et al. Over 26% efficiency SHJ Solar Cells using Nano-crystalline Silicon Layer, *Proc. WCPEC-8, Milan*, Paper 1CP.2.2 (2022) (see also: At 26.81%, LONGi sets a new world record efficiency for silicon solar cells. Press Release, 19 November 2022. [https://www.longi.com/en/news/propelling-the-transformation/.](https://www.longi.com/en/news/propelling-the-transformation/))
- Moslehi MM, Kapur P, Kramer J, et al. World-record 20.6% efficiency 156 mm x 156 mm full-square solar cells using low-cost kerfless ultrathin epitaxial silicon & porous silicon lift-off technology for industry-leading high-performance smart PV modules. *PV Asia Pacific Conference (APVIA/PVAP)*, 24 October 2012.
- Keever MJ, Young TL, Schubert U, Green MA. 10% efficient CSG minimodules. 22nd European Photovoltaic Solar Energy Conference, Milan, 2007.
- Kayes BM, Nie H, Twist R, et al. 27.6% conversion efficiency, a new record for single-junction solar cells under 1 sun illumination. *Proceedings of the 37th IEEE Photovoltaic Specialists Conference*, 2011.
- Venkatasubramanian R, O'Quinn BC, Hills JS, et al. 18.2% (AM1.5) efficient GaAs solar cell on optical-grade polycrystalline Ge substrate. Conference Record, 25th IEEE Photovoltaic Specialists Conference, Washington, 1997; 31–36.
- Wanlass M. Systems and methods for advanced ultra-high-performance InP solar cells. US Patent 9,590,131 B2, 7 March 2017.
- Nakamura M, Yamaguchi K, Kimoto Y, Yasaki Y, Kato T, Sugimoto H. Cd-free Cu (In,Ga)(Se,S)₂ thin-film solar cell with a new world record efficacy of 23.35%, 46th IEEE PVSC, Chicago, IL, June 19, 2019, (see also http://www.solar-frontier.com/eng/news/2019/0117_press.html)
- Diermann R. Avancis claims 19.64% efficiency for CIGS module, *PV Magazine International*, March 4, 2021, (<https://www.pv-magazine.com/2021/03/04/avancis-claims-19-64-efficiency-for-cigs-module/>).
- First Solar Press Release, First Solar builds the highest efficiency thin film PV cell on record, 5 2014.
- Zhou J, Xu X, Wu H, et al. Control of the phase evolution of kesterite by tuning of the selenium partial pressure for solar cells with 13.8% certified efficiency. *Nat Energy*. 2023;8(5):526–535. doi:10.1038/s41560-023-01251-6
- Yan C, Huang J, Sun K, et al. Cu₂ZnSn S₄ solar cells with over 10% power conversion efficiency enabled by heterojunction heat treatment. *Nat Energy*. 2018;3(9):764–772. doi:10.1038/s41560-018-0206-0
- Matsui T, Bidiville A, Sai H, et al. High-efficiency amorphous silicon solar cells: impact of deposition rate on metastability. *Appl Phys Lett*. 2015;106(5):053901. doi:10.1063/1.4907001
- Sai H, Matsui T, Kumagai H, Matsubara K. Thin-film microcrystalline silicon solar cells: 11.9% efficiency and beyond. *Appl Phys Expr*. 2018; 11(2):022301. doi:10.7567/APEX.11.022301
- Park SM, Wei M, Xu J, et al. Engineering ligand reactivity enables high-temperature operation of stable perovskite solar cells. *Science* 2023;381(6654):209–215. doi:10.1126/science.ad4107
- Ding B, Yi Zhang Y, Yong Ding Y, et al. Development of Efficient and Stable Perovskite Solar Cells and Modules. Fifth International Conference on Materials & Environmental Science (ICMES-2022), 2022 Saïdia, Morocco, 12, 46. doi:10.1002/aenm.202202189
- Han L, Fukui A, Chiba Y, et al. Integrated dye-sensitized solar cell module with conversion efficiency of 8.2%. *Appl Phys Lett*. 2009; 94(1):013305. doi:10.1063/1.3054160
- Komiya R, Fukui A, Murofushi N, Koide N, Yamanaka R, Katayama H. Improvement of the conversion efficiency of a monolithic type dye-sensitized solar cell module. Technical Digest, 21st International

- Photovoltaic Science and Engineering Conference, Fukuoka, 2011; 2C-50-08.
21. Würfel U, Herterich J, List M, et al. A 1 cm² organic solar cell with 15.2% certified efficiency: detailed characterization and identification of optimization potential. *Sol RRL*. 2021;5:2000802. doi:10.1002/solr.202000802
 22. <https://www.pv-magazine.com/2021/03/17/organic-pv-module-with-12-36-efficiency/>
 23. https://www.encl.de/fileadmin/user_upload/PR_opv-record_.pdf (accessed 11 November, 2019).
 24. Boyd CC, Cheacharoen R, Leijtens T, McGehee MD. Understanding degradation mechanisms and improving stability of perovskite photovoltaics. *Chem Rev*. 2019;119(5):3418-3451. doi:10.1021/acs.chemrev.8b00336
 25. Yang Y, You J. Make perovskite solar cells stable. *Nature*. 2017; 544(7649):155-156. doi:10.1038/544155a
 26. Krašovec UO, Bokalič M, Topič M. Ageing of DSSC studied by electroluminescence and transmission imaging. *Sol Energy Mater Sol Cell*. 2013;117:67-72. doi:10.1016/j.solmat.2013.05.029
 27. Tanenbaum DM, Hermenau M, Voroshazi E, et al. The ISOS-3 interlaboratory collaboration focused on the stability of a variety of organic photovoltaic devices. *RSC Adv*. 2012;2(3):882-893. doi:10.1039/C1RA00686J
 28. Krebs FC (ed). Stability and degradation of organic and polymer solar cells, Wiley, Chichester, 2012; Jorgensen M, Norrman K, Gevorgyan SA, Tromholt T, Andreasen B, Krebs FC. Stability of polymer solar cells. *Adv Mater*. 2012;24(5):580-612. doi:10.1002/adma.201104187
 29. Green MA. The passivated emitter and rear cell (PERC): from conception to mass production. *Sol Energy Mater sol Cells*. 2015;143:190-197. doi:10.1016/j.solmat.2015.06.055
 30. Richter A, Benick J, Feldmann F, Fell A, Hermle M, Glunz SW. N-type Si solar cells with passivating electron contact: identifying sources for efficiency limitations by wafer thickness and resistivity variation. *Sol Energy Mater sol Cells*. 2017;173:96-105. doi:10.1016/j.solmat.2017.05.042
 31. Yoshikawa K, Kawasaki H, Yoshida W, et al. Silicon heterojunction solar cell with interdigitated back contacts for a photoconversion efficiency over 26%. *Nat Energy*. 2017;2(5):17032. doi:10.1038/nenergy.2017.32
 32. Haase F, Klamt C, Schäfer S, et al. Laser contact openings for local poly-Si-metal contacts enabling 26.1%-efficient POLO-IBC solar cells. *Sol Energy Mater sol Cells*. 2018;186:184-193. doi:10.1016/j.solmat.2018.06.020
 33. Wang Q. Status of Crystalline Silicon PERC Solar Cells. NIST/UL Workshop on Photovoltaic Materials Durability, Gaithersburg, MD USA, 2019, 13, 1, 15, doi:10.17925/HI.2019.13.1.15
 34. <https://taiyangnews.info/technology/jinkosolar-record-25-25-efficiency-for-n-type-mono-cell/>
 35. LONGi achieves new world record for p-type solar cell efficiency. Press Release: 20 September 2022. <https://www.longi.com/en/news/p-type-hjt-record/>
 36. NREL, private communication, 22 May 2019.
 37. https://www.de.uni.lu/forschung/fstm/dphym/news_events/physics_colloquium_state_of_the_art_and_future_prospects_of_thin_film_cigs_solar_cells_invited_speaker_prof_marika_edoff_from_uppsala_university
 38. First Solar Press Release. First Solar Achieves yet another cell conversion efficiency world record, 2016.
 39. Cui X, Sun K, Huang J, et al. Cd-free Cu₂ZnSnS₄ solar cell with an efficiency greater than 10% enabled by Al₂O₃ passivation layer. *Energ Environ Sci*. 2019;12(9):2751-2764. doi:10.1039/C9EE01726G
 40. Peng W, Mao K, Cai F, et al. Reducing nonradiative recombination in perovskite solar cells with a porous insulator contact. *Science*. 2023; 379(6633):683-690. doi:10.1126/science.ade3126
 41. Zhu L, Ming Z, Xu J, et al. Single-junction organic solar cells with over 19% efficiency enabled by a refined double-fibril network morphology. *Nat Mater*. 2022;21(6):656-663. doi:10.1038/s41563-022-01244-y
 42. Ren Y, Zhang D, Suo J, et al. Hydroxamic acid pre-adsorption raises the efficiency of cosensitized solar cells. *Nature*. 2023;613(7942):60-65. doi:10.1038/s41586-022-05460-z
 43. Sasaki K, Agui T, Nakaido K, Takahashi N, Onitsuka R, Takamoto T. Proceedings, 9th International Conference on Concentrating Photovoltaics Systems, Miyazaki, Japan 2013.
 44. Schygulla P, Müller R, Höhn O, et al. Wafer-Bonded Two-Terminal III-V//Si Triple-Junction Solar Cell with Power Conversion Efficiency of 36.1% at AM1.5g. Presented at the 40th EU PVSEC, Lisbon, 2023, Paper 2DO.9 (submitted to *Prog. Photovolt. Res. Appl.*).
 45. Essig S, Allebé C, Remo T, et al. Raising the one-sun conversion efficiency of III-V/Si solar cells to 32.8% for two junctions and 35.9% for three junctions. *Nat Energy*. 2017;2:17144. doi:10.1038/nenergy.2017.144
 46. Feifel M, Lackner D, Schön J, et al. Epitaxial GaInP/GaAs/Si triple-junction solar cell with 25.9% AM1.5g efficiency enabled by transparent metamorphic Al_xGa_{1-x}As_yP_{1-y} step-graded buffer structures. *Sol RRL*. 2021;5(5):2000763. doi:10.1002/solr.202000763
 47. Grassman TJ, Chmielewski DJ, Carnevale SD, Carlin JA, Ringel SA. GaAs_{0.75}P_{0.25}/Si dual-junction solar cells grown by MBE and MOCVD. *IEEE J Photovoltaics*. 2016;6(1):326-331. doi:10.1109/JPHOTOV.2015.2493365
 48. Green MA, Keevers MJ, Concha Ramon B, et al. Improvements in sunlight to electricity conversion efficiency: above 40% for direct sunlight and over 30% for global. Paper 1AP.1.2, *European Photovoltaic Solar Energy Conference 2015*, Hamburg, 2015.
 49. <https://www.longi.com/en/news/new-conversion-efficiency/>
 50. <https://www.oxfordpv.com/oxford-pv-story>
 51. Yamamoto K, Mishima R, Uzu H, Adachi D. High efficiency perovskite/heterojunction crystalline silicon tandem solar cells: towards industrial-sized cell and module. *Jpn J Appl Phys*. 2023; 62(SK):SK1021. doi:10.35848/1347-4065/acc593
 52. Jošt M, Köhnen E, Al-Ashouri A, et al. Perovskite/CIGS tandem solar cells: from certified 24.2% toward 30% and beyond. *ACS Energy Lett*. 2022;7(4):1298-1307. doi:10.1021/acseenergylett.2c00274
 53. Lin R, Xu J, Wei MY, et al. All-perovskite tandem solar cells with improved grain surface passivation. *Nature*. 2022;603(7899):73-78. doi:10.1038/s41586-021-04372-8
 54. Xiao K, Lin YH, Zhang M, et al. Scalable processing for realizing 21.7%-efficient all-perovskite tandem solar modules. *Science*. 2022; 376(6594):762-767. doi:10.1126/science.abn7696
 55. Sai H, Matsui T, Koida T, Matsubara K. Stabilized 14.0%-efficient triple-junction thin-film silicon solar cell. *Appl Phys Lett*. 2016; 109(18):183506. doi:10.1063/1.4966996
 56. Matsui T, Maejima K, Bidiville A, et al. High-efficiency thin-film silicon solar cells realized by integrating stable a-Si:H absorbers into improved device design. *Jpn J Appl Phys*. 2015;54:08KB10. doi:10.7567/JJAP.54.08KB10
 57. <http://mldevices.com/index.php/news/> (accessed 28 October 2018).
 58. Geisz JF, Steiner MA, Jain N, et al. Building a six-junction inverted metamorphic concentrator solar cell. *IEEE J Photovoltaics*. 2018;8(2): 626-632. doi:10.1109/JPHOTOV.2017.2778567
 59. Makita K, Kamikawa Y, Mizuno H, et al. III-V//Cu_xIn_{1-y}Ga_ySe₂ multijunction solar cells with 27.2% efficiency fabricated using modified smart stack technology with Pd nanoparticle array and adhesive material. *Prog Photovolt Res Appl*. 2021;29(8):887-898. doi:10.1002/pip.3398
 60. <https://www.hanwha-qcells.com> (accessed 28 October 2019).
 61. Mattos LS, Scully SR, Syfu M, et al. New module efficiency record: 23.5% under 1-sun illumination using thin-film single-junction GaAs solar cells. *Proceedings of the 38th IEEE Photovoltaic Specialists Conference*, 2012.

62. Sugimoto H. High efficiency and large volume production of CIS-based modules. 40th IEEE Photovoltaic Specialists Conference, Denver, 2014.
63. <http://www.firstsolar.com/en-AU/-/media/First-Solar/Technical-Documents/Series-6-Datasheets/Series-6-Datasheet.ashx> (accessed 28 October 2019).
64. Cashmore JS, Apolloni M, Braga A, et al. Improved conversion efficiencies of thin-film silicon tandem (MICROMORPH™) photovoltaic modules. *Sol Energy Mater sol Cells*. 2016;144:84-95. doi:10.1016/j.solmat.2015.08.022
65. Higuchi H, Negami T. Largest highly efficient 203 x 203 mm² CH₃NH₃PbI₃ perovskite solar modules. *Jpn J Appl Phys*. 2018; 57(8S3):08RE11. doi:10.7567/JJAP.57.08RE11
66. Hosoya M, Oooka H, Nakao H, et al. Organic thin film photovoltaic modules. *Proceedings of the 93rd Annual Meeting of the Chemical Society of Japan* 2013; 21-37.
67. Sharp Achieves World's Highest¹ Conversion Efficiency of 32.65%² in a Lightweight, Flexible, Practically Sized Solar Module. Press Release: June 6, 2022. <https://global.sharp/corporate/news/220606-a.html>
68. Bheemreddy V, Liu BJJ, Wills A, Murcia CP. Life prediction model development for flexible photovoltaic modules using accelerated damp heat testing. *IEEE 7th World Conf. on Photovoltaic Energy Conversion (WCPEC)* 2018: 1249-1251.
69. Takamoto T, Juso H, Ueda K, et al. IMM Triple-junction Solar Cells and Modules optimized for Space and Terrestrial Conditions. *Proceedings of the 44th IEEE Photovoltaic Specialist Conference (PVSC)*, 2017 doi:10.1109/PVSC.2017.8366097.
70. Slade A, Garboushian V. 27.6% efficient silicon concentrator cell for mass production. Technical Digest, 15th International Photovoltaic Science and Engineering Conference, Shanghai, 2005; 701.
71. Ward JS, Ramanathan K, Hasoon FS, et al. A 21.5% efficient cu (in,Ga)Se₂ thin-film concentrator solar cell. *Prog Photovolt: Res Appl*. 2002;10(1):41-46. doi:10.1002/pip.424
72. Dimroth F, Tibbits TND, Niemeyer M, et al. Four-junction wafer-bonded concentrator solar cells. *IEEE J Photovolt*. 2016;6(1):343-349. doi:10.1109/JPHOTOV.2015.2501729
73. NREL Press Release NR-4514, 16 2014.
74. Press Release, Sharp Corporation, 2012 (accessed at <http://sharp-world.com/corporate/news/120531.html> on 5 June 2013).
75. Jain N, Schulte KL, Geisz JF, et al. High-efficiency inverted metamorphic 1.7/1.1 eV GaInAsP/GaInAs dual-junction solar cells. *Appl Phys Lett*. 2018;112(5):053905. doi:10.1063/1.5008517
76. Steiner M, Siefert G, Schmidt T, Wiesenfarth M, Dimroth F, Bett AW. 43% sunlight to electricity conversion efficiency using CPV. *IEEE J Photovolt*. 2016;6(4):1020-1024. doi:10.1109/JPHOTOV.2016.2551460
77. Green MA, Keevers MJ, Thomas I, Lasich JB, Emery K, King RR. 40% efficient sunlight to electricity conversion. *Prog Photovolt: Res Appl*. 2015;23(6):685-691. doi:10.1002/pip.2612
78. Chiang CJ, Richards EH. A 20% efficient photovoltaic concentrator module. *Conf. Record, 21st IEEE Photovoltaic Specialists Conference*, Kissimmee, 1990: 861-863.
79. <http://amonix.com/pressreleases/amonix-achieves-world-record-359-module-efficiency-rating-nrel-4> (accessed 23 October 2013).
80. van Riesen S, Neubauer M, Boos A, et al. New module design with 4-junction solar cells for high efficiencies. *Proceedings of the 11th Conference on Concentrator Photovoltaic Systems*, 2015.
81. Martínez JF, Steiner M, Wiesenfarth M, Siefert G, Glunz SW, Dimroth F. Power rating procedure of hybrid CPV/PV bifacial modules. *Prog Photovolt Res Appl*. 2021;29(6):614-629. doi:10.1002/pip.3410
82. Zhang F, Wenham SR, Green MA. Large area, concentrator buried contact solar cells. *IEEE Trans Electron Devices*. 1995;42(1):144-149. doi:10.1109/16.370024
83. Slooff LH, Bende EE, Burgers AR, et al. A luminescent solar concentrator with 7.1% power conversion efficiency. *Phys Stat sol (RRL)*. 2008;2(6):257-259. doi:10.1002/pssr.200802186
84. Steiner M, Wiesenfarth M, Martínez JF, Siefert G, Dimroth F. Pushing energy yield with concentrating photovoltaics, AIP Conference Proceedings 2149, 060006 2019 10.1063/1.5124199.
85. Mülleijans H, Winter S, Green MA, Dunlop ED. What is the correct efficiency for terrestrial concentrator PV devices? *38th European Photovoltaic Solar Energy Conference*, Sept. 2021 (accepted for presentation).
86. Gueymard CA, Myers D, Emery K. Proposed reference irradiance spectra for solar energy systems testing. *Solar Energy*. 2002;73(6): 443-467. doi:10.1016/S0038-092X(03)00005-7
87. Program milestones and decision points for single junction thin films. *Annual Progress Report 1984, Photovoltaics, Solar Energy Research Institute, Report DOE/CE-0128*, 1985, 7.
88. Sakata I, Tanaka Y, Koizawa K. Japan's New National R&D Program for Photovoltaics. *Photovoltaic Energy Conversion, Conference Record of the 2006 IEEE 4th World Conference*, 2008; 1: 1-4.
89. Jäger-Waldau A (Ed). *PVNET: European Roadmap for PV R&D*, EUR 21087 EN. Vol. 451-452; 2004:448-454. doi:10.1016/j.tsf.2003.10.140

How to cite this article: Green MA, Dunlop ED, Yoshita M, et al. Solar cell efficiency tables (Version 63). *Prog Photovolt Res Appl*. 2024;32(1):3-13. doi:10.1002/pip.3750